

Daniel C. Lee, Neil R. Chatterjee, and Timothy J. Carroll

**Abstract**

Myocardial perfusion is an important measurement in the diagnosis and management of coronary artery disease. While clinical measurement of myocardial perfusion has long been dominated by nuclear imaging, MRI has recently emerged as an alternative method with many significant advantages. Compared to single photon emission computed tomography (SPECT), MRI has much higher resolution, requires no radiation dose, and has the potential for more quantitative measurements. MR perfusion measurement can be complex, however, and when designing an MR perfusion experiment there are a variety of choices to consider. Unfortunately, there is no consensus MRI perfusion implementation that is best for all situations, and choosing the ideal parameters for a given scan requires a careful understanding of the pros and cons of each component of an MRI perfusion experiment. In this chapter, we discuss the different components of cardiac perfusion MRI including pulse sequences, image readout, acceleration techniques, and image analysis. In each section, we review the basic theory behind each technique and then discuss their relative advantages and disadvantages. We conclude with a brief discussion of emerging techniques that are currently being researched.

**Keywords**

MRI • CMR • Perfusion • Blood flow • Pulse sequences • Quantification

**Introduction**

Imaging myocardial perfusion, the amount of blood flow within heart muscle, plays a critical role in diagnosing coronary artery disease, making revascularization decisions, and

predicting a patient's future risk of a cardiac event. In addition to its role in coronary artery disease, abnormalities in myocardial perfusion have also been identified in other diseases such as cardiomyopathy [1], repaired coarctation of the aorta [2], and asymptomatic individuals with variable atherosclerosis risk factors [3].

---

D.C. Lee, MD (✉)  
Division of Cardiology, Department of Medicine, Northwestern  
University Feinberg School of Medicine, Chicago, IL, USA  
e-mail: [dlee@northwestern.edu](mailto:dlee@northwestern.edu)

N.R. Chatterjee, BS  
Northwestern University Feinberg School of Medicine,  
Chicago, IL, USA  
e-mail: [neil-chatterjee@northwestern.edu](mailto:neil-chatterjee@northwestern.edu)

T.J. Carroll, PhD  
Department of Radiology, Northwestern Memorial Hospital,  
Chicago, IL, USA  
e-mail: [t-carroll@northwestern.edu](mailto:t-carroll@northwestern.edu)

The clinical measurement of myocardial perfusion has long been dominated by nuclear imaging -principally single photon emission computed tomography (SPECT) [4]. More recently, MRI has emerged as an alternative way to measure cardiac perfusion. MRI has significant advantages over SPECT including much higher resolution (Fig. 13.1), no required radiation dose, and the potential for more quantitative measurements. MRI measurement of myocardial perfusion has been the subject of much research and has been described in a number of review articles [5–9].

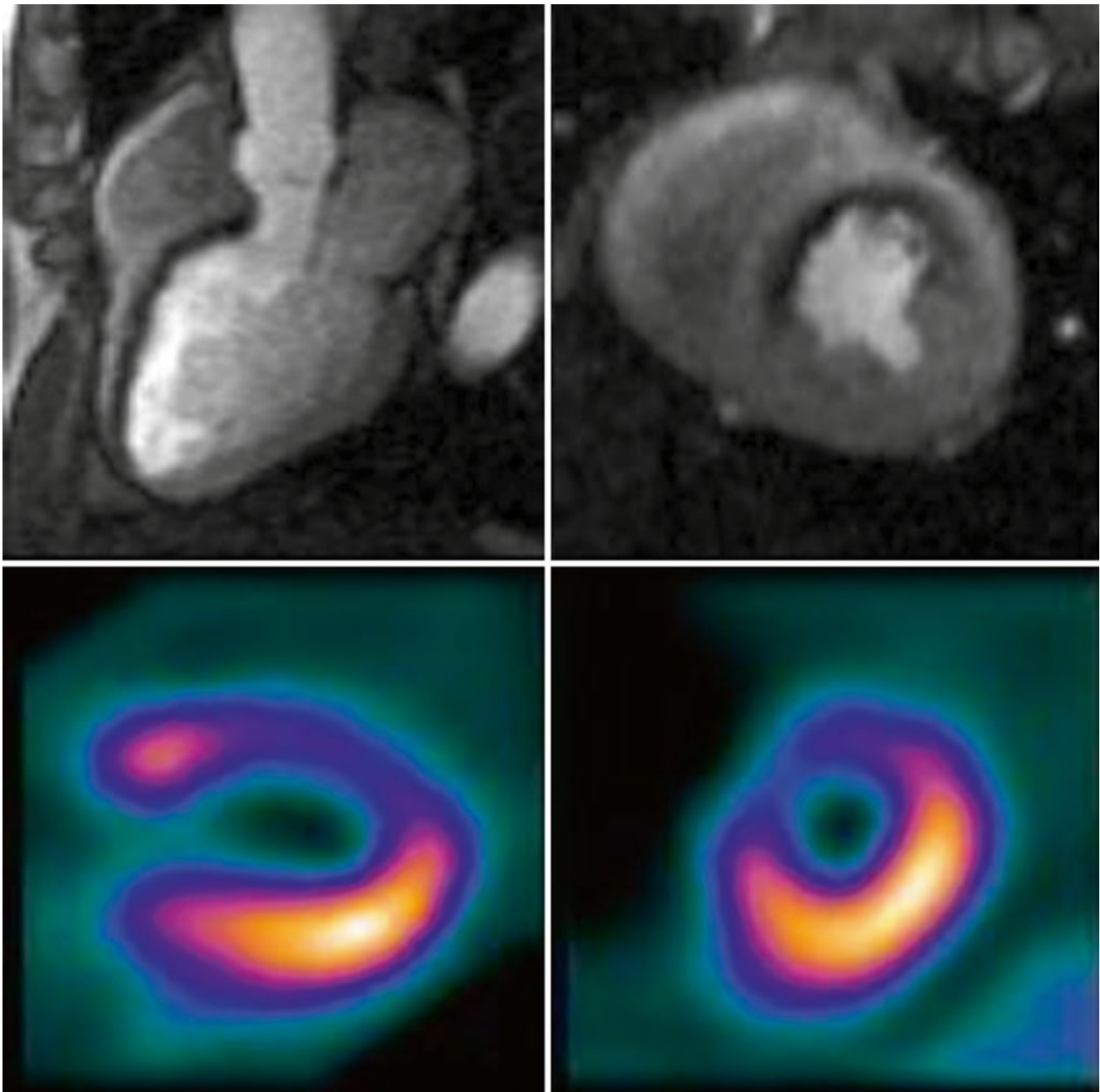


**Fig. 13.1** Severe ischemia in the distribution of the left anterior descending coronary artery seen by MR perfusion (*top row*) and SPECT imaging (*bottom row*). A single frame from the first-pass MR perfusion series demonstrates severe ischemia of the anteroseptum from base to

apex in the three-chamber view (*top left*) and of the septal and anterior walls in the mid-chamber short axis view (*top right*). On SPECT imaging, a similar distribution of ischemia is seen on the vertical long axis (*bottom left*) and mid-chamber short axis view (*bottom right*)

The most common way to measure perfusion with CMR is via the “first pass” technique. A bolus of contrast is injected in a peripheral vein, and contrast enhancement is observed as the bolus passes through the myocardium. Mathematical analysis of the shape of the time-signal intensity curve measured in the myocardium is used to quantify the tissue perfusion in ml/g-min. There are other techniques for measuring perfusion with MRI, but they

have notable drawbacks. Arterial spin labeling (ASL) [10] is a promising technique that uses no exogenous contrast, but has less contrast to noise ratio (CNR) than traditional first pass methods. Blood Oxygen Level Dependent (BOLD) imaging [11] also uses no exogenous contrast, but its interpretation for quantitative perfusion can be complicated because it also depends on factors such as oxygen extraction fraction. Because first pass with a contrast bolus

makes up the overwhelming majority of cardiac perfusion scans, it will be the focus of this chapter.

## Pulse Sequences

### Constraints and Requirements

The choice of which pulse sequence to use is a key determinant of image contrast, spatial and temporal resolution, coverage, and degree of artifacts. These characteristics are usually at odds with one another – for example gains in contrast may come at the expense resolution or coverage – and selecting the optimal sequence requires weighing these competing gains and losses against each other. Consequently, when selecting a perfusion sequence, it is critical to consider the basic requirements for cardiac perfusion imaging. These are:

1. **Strong  $T_1$  contrast.** The contrast agent used in MRI perfusion significantly alters the  $T_1$  of the myocardium during first pass, therefore  $T_1$  sensitive image contrast is desirable.
2. **Coverage of relevant myocardium.** Usually this includes at minimum one short axis slice each through the base, middle, and apex of the myocardium of the left ventricle (LV).
3. **Spatial Resolution.** At minimum, most sequences must be able to distinguish between subendocardial and transmural ischemia.
4. **Temporal Resolution.** To adequately sample flow at the myocardial level, images must be acquired every one to two heartbeats. For quantitative perfusion, there is the additional requirement of being able to adequately sample the input function within the blood pool of the LV. Because contrast passes much quicker through the LV than the myocardium, this usually requires sampling every heartbeat.
5. **Lack of Artifacts.** In particular, the dark rim artifact is a specific property of MRI perfusion images that can mimic perfusion defects resulting in potential for misinterpretation and should be minimized.

In meeting these requirements, perfusion imaging has a critical constraint that is absent in much of CMR: because characterizing the bolus passage requires acquiring a full image every one to two heart beats, segmented acquisition (as is used in Cine and Late Gadolinium Enhanced imaging) is limited or impossible. In order to achieve full heart coverage, typically three short axis images must be acquired within the time course of a single heartbeat. This limits perfusion imaging to very time-efficient pulse sequences that reduce the time to acquire an image to ~100 ms. The image

acquisition time is determined by the length of the cardiac cycle which is often shortened by vasodilator stress.

### Preparation Pulses

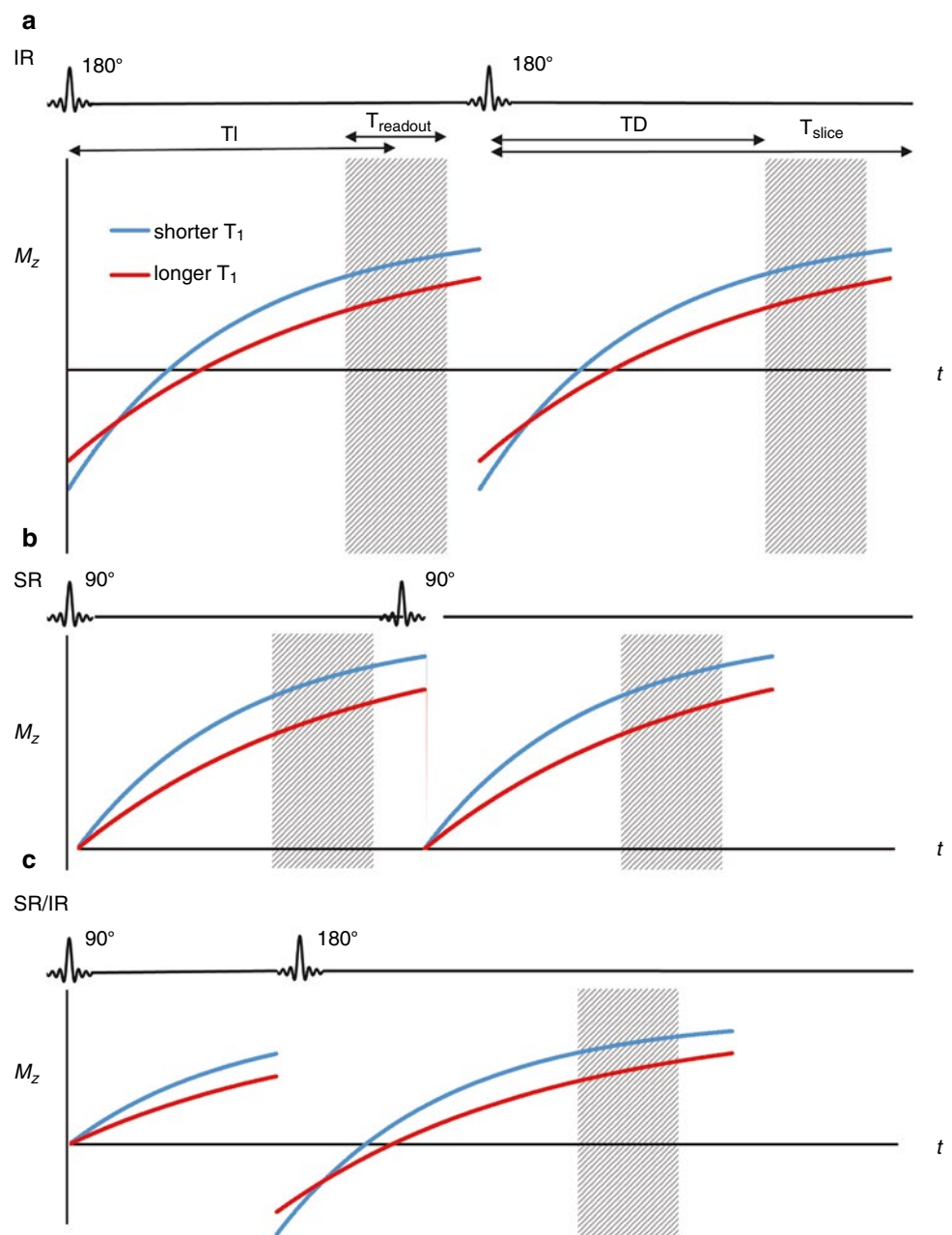
At the most basic level, a  $T_1$ -weighted image is acquired by perturbing the longitudinal magnetization ( $M_z$ ) away from equilibrium through the application of an RF pulse at the beginning of the pulse sequence and then acquiring images before the magnetization has a chance to return to normal. As a general rule, blood, fat, and myocardium with short  $T_1$  will return to its unperturbed state faster, appearing bright in a  $T_1$ -weighted images. There are two approaches to perturb  $M_z$  in cardiac perfusion imaging: with a  $180^\circ$  (i.e. an inversion) RF pulse in inversion recovery (IR) exams and a  $90^\circ$  RF pulse which completely eliminates or “saturates” MRI signal in a so-called saturation recovery (SR) exam. The SR and IR pulses are often referred to as magnetization preparation pulses and are separate from the RF pulses played during the image acquisition or image “readout”, both of which must be considered in the optimization of a cardiac perfusion exam.

Historically, IR was used for CMR perfusion. Because IR is a  $180^\circ$  pulse, it has the potential for the most dynamic range and hence most contrast (Fig. 13.2). However,  $M_z$  after the pulse is dependent on  $M_z$  immediately prior to the pulse (it will be the same magnitude but point in the opposite direction). This means that the length of the previous TR will affect the magnitude of  $M_z$  after inversion pulse. In a gated cardiac scan, the TR is roughly equal to the RR interval. This makes scans with IR preparation very sensitive to changes in heart rate and arrhythmias because the RR and TR change throughout the scan. The other disadvantage of IR is that it requires a longer readout because it takes longer for the magnetization to recover. Practically, this means that more time is required per slice, so fewer slices can be acquired, and there is a decrease in spatial coverage.

Currently, the majority of CMR perfusion scans are acquired using SR preparation. While there is less dynamic range and contrast because it is only a  $90^\circ$  pulse (see Fig. 13.2), SR does not have the other drawbacks of IR. Critically, SR pulses will always set  $M_z$  to zero regardless of the prior  $M_z$ , so the signal has no heart rate dependence. Additionally, because the readout is faster, more slices can be acquired allowing for greater spatial coverage.

Other pulse preparations are currently being developed. Some, like magnetization driven steady state, offer better linearity at the expense of CNR, which may be useful for some quantification applications. Others are a hybrid of SR and IR preparations. For example, an SR prep followed by an IR prep [12] will exhibit some characteristics of each. There will be no heart rate dependence, and CNR will be improved

**Fig. 13.2** (a) Saturation recovery (SR), (b) inversion recovery (IR), and (c) hybrid SR-IR preparations for myocardial imaging. IR has a greater signal range but is slower and is susceptible to variations in heart rate (note that  $M_z$  after the inversion pulse is dependent on  $T_{\text{slice}}/T_1$ ). For the hybrid SR-IR, the initial SR preparation removes any heart rate variability, and the following IR pulse increases signal range over an SR only prep.  $TD$  trigger delay,  $TI$  inversion time (time from preparation to center of k-space),  $T_{\text{readout}}$  total time for acquisition of all k-space data for a single slice,  $T_{\text{slice}}$  total time required for acquiring a single slice. Note that  $TI$  is  $TD$  plus half  $T_{\text{readout}}$



over a simple SR prep, but readout would take even longer and coverage would decrease. This could be used in cases where good CNR is important but coverage is not (e.g. a diffuse process like systemic sclerosis).

For a  $90^\circ$  SR preparation, there are a few different choices for how to implement the RF pulse. A rectangular pulse is the simplest, however in the presence of any  $B_1$  field inhomogeneity (common in cardiac imaging) a rectangular pulse will result in incomplete saturation. Other RF pulses have been designed that have improved performance in the presence of  $B_1$  inhomogeneity. Two important ones are adiabatic pulses [13] and rectangular pulse trains [14]. Both of these show markedly improved saturation (Fig. 13.3) [6, 14].

However their drawbacks are longer pulse durations and higher SAR. The longer pulse duration is minor compared the image acquisition time ( $\sim 8$  ms compared to  $\sim 150$ – $200$  ms), but additional SAR can be problematic with large coverage at higher field strengths (3 T).

### Image Readout: Snapshot FLASH, SSFP, GRE-EPI

Each type of magnetization preparation pulse can be combined with different types of image readout. The most common types are ultra fast gradient echo (e.g. TurboFLASH,

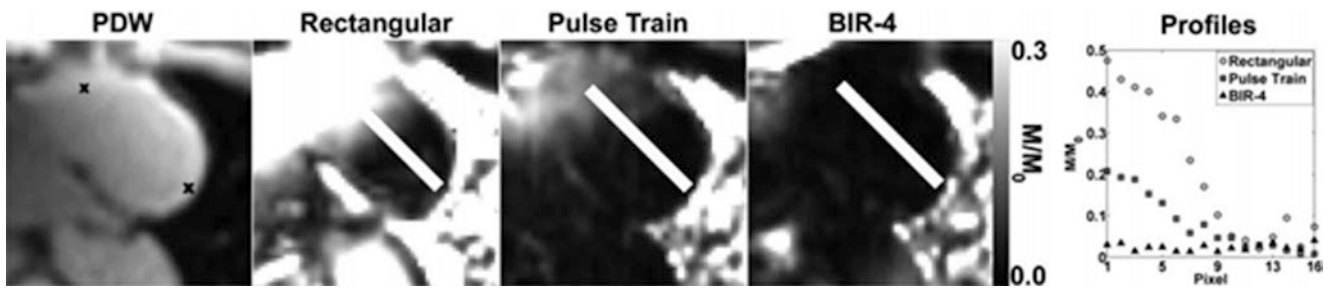


**Fig. 13.3** Short axis images demonstrating saturation inhomogeneity with different types of SR preparation pulses. “x” marks on the PDW image mark the end points of the measured signal intensity. For complete homogeneous saturation, the signal should be zero across the

entire line. The pulse train shows improved homogeneity over a simple rectangular pulse, and the BIR-4 adiabatic pulse is even more homogeneous (Reproduced from Kim et al. [14], with permission of John Wiley & Sons)

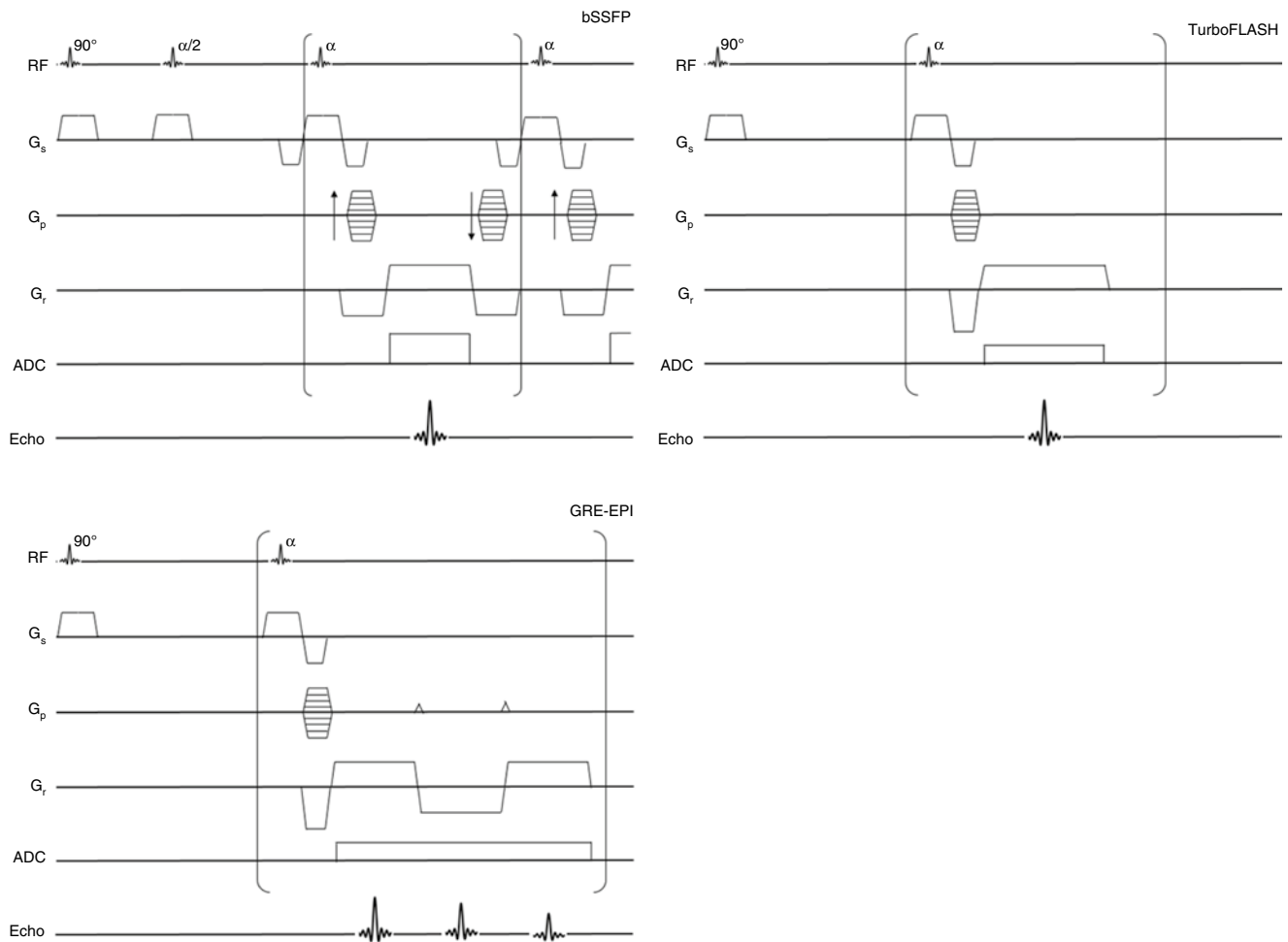


**Fig. 13.4** Pulse sequence diagrams for bSSFP, FLASH, and GRE-EPI readouts

fast GRE, and Turbo Field Echo) [15], gradient echo with echo planar readout (GRE-EPI) [16], or steady state free precession (SSFP – termed TrueFISP, FIESTA, balanced FFE by various vendors) [17], and despite much debate, there is no clear consensus for which sequence is best for CMR perfusion and is usually determined based on the preference of the physician.

Fast Low Angle Shot (FLASH) was one of the first available rapid imaging sequences. With FLASH, each line in k-space is preceded by a low flip angle excitation and then any transverse magnetization at the end of the readout is spoiled before moving to the next line (Fig. 13.4). Since each line has its own excitation, the imaging time for the readout (not including preparation) will be  $T_{\text{readout}} = TR * N_{\text{phase}}$ . E.g.

for a  $128 \times 80$  matrix at  $TR = 2$  ms, the readout time would be 160 ms. (Note:  $TR$  here refers to time between excitations during the readout, it does not refer to the time between successive image acquisitions.) TurboFLASH is a variation on FLASH with very short  $TR$  and low flip angle. As a consequence, TurboFLASH is predominantly proton density weighted instead of having the typical  $T_1$  FLASH weighting. However, with IR or SR prep a TurboFLASH sequence will have  $T_1$  weighting.

GRE-EPI is similar to FLASH, except that instead of reading out one line of  $k$ -space per acquisition, multiple lines are read out. This means that fewer excitations are needed during readout, which makes GRE-EPI more efficient and hence faster than FLASH. The number of lines read per excitation is referred to as the echo train length (ETL). For GRE-EPI, the readout time will instead be  $T_{\text{readout}} = TR * N_{\text{phase}} / \text{ETL}$ . For example a  $128 \times 80$  matrix at  $TR = 6$  ms with an ETL of 4, the readout time would be  $80 * 6 / 4 = 120$  ms. The imaging readout time is particularly important in CMR because motion artifacts are reduced with shorter readout times. This makes GRE-EPI less sensitive to motion than FLASH. Additionally, the faster readout time reduces the overall imaging time per slice, which means more slices can be acquired during each heartbeat. One drawback of GRE-EPI, however, is that magnetic field imperfections accumulate through the extended readout. The accumulation of error manifests itself as additional phase, which can mimic the intended phase used to localize signal within an image. The result is that EPI images can exhibit phase related “ghosting” artifacts.

Steady State Free Precession (SSFP) images are a variant of FLASH. Unlike in FLASH, in SSFP, transverse magnetization ( $M_{x-y}$ ) is not eliminated before the next excitation. Rather than being destroyed (i.e. spoiled) by the application of phase-modulated RF pulses or large field gradients, the residual transverse magnetization is refocused and combined with newly excited transverse excitation to dramatically increase the magnetization used in the formation of an image (Fig. 13.4). This gives SSFP greater SNR than either FLASH or GRE-EPI. Also, because initial magnetization depends on both the longitudinal magnetization and the refocused transverse magnetization, SSFP will have some  $T_2$  as well as  $T_1$  contrast. This makes TE particularly important for SSFP readouts. Like FLASH, SSFP requires one excitation per readout line, and has comparable readout times. Some studies have found more dark rim artifacts with SSFP [18, 19]. Magnetic field inhomogeneity, which can be problematic in the chest where the lungs impart large local magnetic susceptibility changes, is also a problem in SSFP readouts, which has limited SSFP adoption at 3 T. It has also been reported that the excitations in SSFP can interfere with accurate ECG gating [17]. Still, in spite of these drawbacks, the gain in SNR has seen SSFP become increasingly popular in CMR perfusion.

Despite multiple studies comparing the above methods, there is no clear-cut consensus as to which is the best method, and each one offers advantages and disadvantages. In a review article, Kellman and Arai compared SSFP, FLASH, and GRE-EPI using state-of-the-art implementations in 2007 [6]. They found that GRE-EPI had the fastest acquisition, but that SSFP has 40 % higher CNR.

## Acquiring Multiple Slices

Typically CMR perfusion scans require multiple slices for adequate coverage of the LV myocardium supplied by the coronary arteries. The most common method for acquiring multiple slices is to use multiple SR preps. The first slice is SR prepped and read out, then the second slice is SR prepped and read out, etc. until all the slices are completed. Another approach is to use a single SR prep and then read out multiple slices. This is faster than using multiple SR preps, so greater spatial coverage is possible. However, the time between the SR prep and readout will be different for each slice. This leads to a very important disadvantage: each slice will have a different TI, so each slice will have different CNR. A third possibility is to use a single SR prep but interleave the slice readouts. This keeps the same efficiency gains but equalizes the TIs, so there is no CNR variation between slices. However, the readout per slice is longer, which increases susceptibility to motion artifacts.

## Acceleration Techniques

Due to the need for very fast image acquisition, cardiac perfusion sequences are almost always run with some sort of acceleration technique. Acceleration techniques include parallel imaging (e.g. SMASH [20], SENSE [21], and GRAPPA [22]),  $k$ -t Blast/ $k$ -t SENSE [23], and HYPR [24, 25]. Much research has been focused on acceleration techniques in recent years, and a multitude of techniques have been developed and compared [26, 27]. In all of these techniques, image acquisition time is reduced by intentionally sampling only a subset of the data needed to create an MRI images. The uncollected or “missing” MRI data are mathematically synthesized using complimentary information collected from different receiver coils. In other words, most acceleration techniques use the spatial location of the acquired signal which is inherent in the receiver coil configuration to reduce the amount of imaging data that must be acquired for artifact free images. Since receiver coil information is acquired simultaneously, i.e. in parallel, the general approach to accelerate is referred to as “parallel imaging”. However, a major tradeoff in all cases is that faster acquisition results in lower SNR. A review of parallel imaging basics can be found by Deshmene et al. [28].

Sensitivity encoding (SENSE) and generalized autocalibrating partially parallel acquisition (GRAPPA) are two widely available methods of parallel imaging, and both have major advantages in that they rely on relatively simple theoretical underpinnings and make very few assumptions about the nature of the underlying images. With parallel imaging, reconstruction additionally incorporates information from multiple independent receiving coils. In essence, spatial information that would otherwise be obtained by spatial encoding via gradients is instead obtained by information in independent coils in the receiver coil array. With SENSE, coil sensitivity profiles are used to unwrap the aliased images in image space. With GRAPPA, the unsampled lines in k-space are calculated by combining information from neighboring lines in multiple coils, and the filled-in k-space is then reconstructed as usual. This eliminates the ghosting artifacts that would normally be seen by undersampling, and the more receiving channels that are used, the more k-space can be undersampled and acquisition speed increased.

Other techniques achieve even greater acceleration by incorporating temporal information. For most rapidly acquired image series of the heart, much of the image remains unchanged between images, and data is correlated in time. k-t BLAST and k-t SENSE are two well-known techniques that take advantage of this correlation by acquiring a training data set (acquired at low resolution and un-aliased) that is used to inform the reconstruction of the sparsely sampled and rapidly acquired data. k-t BLAST does not incorporate coil channel information in its reconstruction and can be used with single channel coils whereas k-t SENSE incorporates coil channel information as well. Compared to standard parallel imaging techniques, k-t BLAST and k-t SENSE are capable of faster imaging, but at the cost of increased noise and more assumptions in the model (e.g. that motion during the training data is representative of motion in the rest of the data).

## Motion Correction

While many cardiac MRI scans rely on breath holds to ensure that there is minimal movement of the heart during the scan, the longer acquisition times of a cardiac perfusion scan (typically 45 s–1.5 min) can make breath holds impractical. As a result, there is usually considerable cardiac motion over the course of a perfusion scan. This is problematic when analyzing perfusion images. Generating signal intensity time curves requires segmenting along the epi- and endocardial borders, but this is an extremely time intensive process to do frame by frame, and automatic segmentation often does not trace the borders well. A more efficient process is to first register all of the images together, draw the contours on a single image,

and then propagate the contours throughout the series and make (relatively minor) adjustments as needed. As such, most cardiac perfusion scans will include some form of motion correction for image registration.

There are a multitude of motion corrections algorithms that have been proposed. Motion can be corrected prospectively using navigator pulses that track the motion of the diaphragm [29]. Motion can also be corrected retrospectively using a variety of methods [30–33]. In practice, many vendors will have some form of inline motion correction included in their cardiac sequences. A comprehensive review of cardiac motion correction can be found in the review by Scott et al. [34].

## Artifacts

There are several artifacts seen in CMR perfusion imaging, and the most important one is the dark rim artifact (DRA) (Fig. 13.5). The DRA manifests as a dark rim that is sometimes seen in the subendocardial border of the ventricle. This ring can easily be mistaken for hypoperfusion and cause incorrect diagnoses, which is why DRA is regarded as the most concerning artifact in CMR. Much research has gone into determining the cause of the DRA, and some common hypotheses include Gibbs ringing, contrast associated susceptibility changes, motion artifacts, and partial volume effects [35]. However, no theory has been clearly identified as the sole cause of DRA, and its origins remain widely debated.

## 1.5 T vs 3 T

While the majority of clinical scanners use 1.5 T magnets, 3 T is becoming increasingly common, and the choice between the two has a significant effect on CMR perfusion. The higher magnetic field of the 3.0 T results in a doubling of the signal-to-noise ratio of images and a 30 % prolongation of  $T_1$  values [36]. Importantly, Gadolinium-based contrast agents have less relaxivity at 3 T. However, since  $T_1$  values are also higher in the blood and myocardium at 3 T than at 1.5 T there is a net increase in  $\Delta T_1$  and gain in CNR [37].

While 3 T offers CNR advantages, it has other disadvantages. Artifacts are more prominent at 3 T, though faster imaging and higher bandwidth can mitigate artifacts at the cost of SNR. Critically for SSFP sequences, there is more inhomogeneity at 3 T [38]. There is also greater energy deposition as quantified by the Specific Absorption Rate (SAR) at 3 T, which limits the TR and flip angles that can be used, and ECG signal is noisier at 3 T, which can influence any scan where accurate gating is critical.

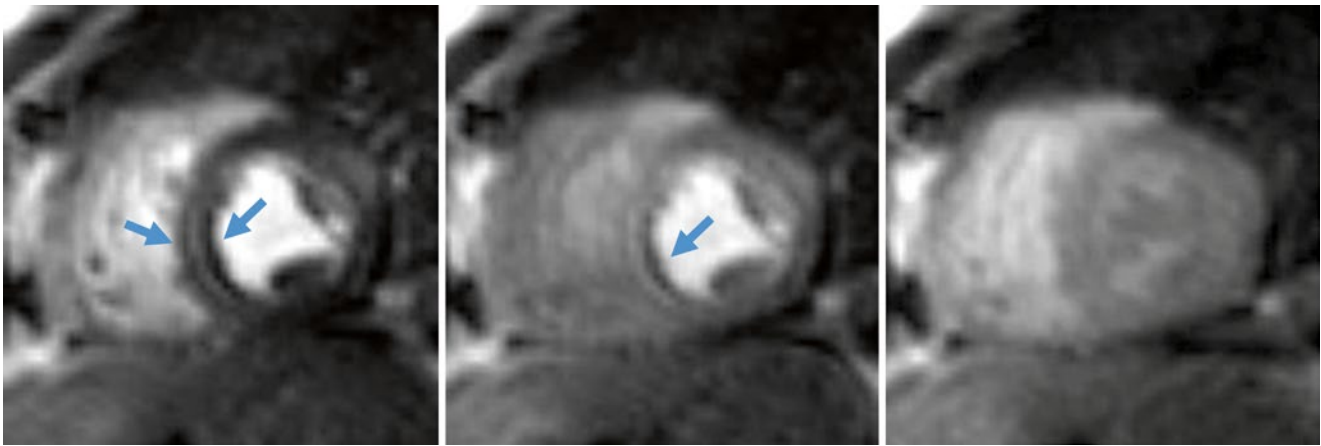


**Fig. 13.5** Dark rim artifact (DRA). Note that the artifact is only apparent when there is contrast in the adjacent ventricle and does not persist after the first-pass

## Summary

There are a multitude of choices available when creating a CMR perfusion sequence. Preparation can be IR, SR, or a hybrid, and there are multiple ways to implement the preparation. Readouts can be some variation of FLASH, GRE-EPI, or SSFP. There is no single best combination for all applications, and selection of the “best” sequence depends on the specific needs of a particular scan. For example, relative to ischemia, post infarction imaging involves more microvascular than macrovascular obstruction, so contrast washes out more slowly [8]. In this case, some temporal resolution could be sacrificed to gain greater spatial resolution to better delineate the size of injured myocardium. Conversely, for a diffuse process like microvascular dysfunction in Syndrome X, spatial coverage could be neglected in favor of having greater spatial resolution in fewer slices to evaluate subendocardial hypoperfusion.

## Image Analysis

For any given image series, there are a multitude of different ways to process the data and provide an assessment of cardiac perfusion. Recent articles have reviewed and compared various methods [8, 9, 39], there is no clear consensus on the best approach. Broadly speaking, perfusion analysis can be categorized as qualitative, semi-quantitative, or absolute quantitative where parametric images present signal intensity in proportion to ml/-g-min of perfusion. Absolute quantification allows a more direct comparison in cross-sectional and longitudinal studies of perfusion changes within individual patients and in patient populations.

## Qualitative

The simplest way of analyzing perfusion data is to simply visually inspect myocardial signal changes as the bolus of contrast agent passes, which is what is done in most clinical applications. A physician will cycle through the perfusion series and watch the myocardium as the contrast flushes through. Any areas that remain dark have less perfusion than the surrounding bright tissue. Comparison of stress, rest, and late gadolinium enhanced images allows defects to be attributed to ischemia, infarction, or artifact. Defects seen at stress but not at rest are interpreted as reversible ischemia. Matched defects seen at stress and rest with a corresponding area of late gadolinium enhancement are interpreted as infarction. Matched defects seen at stress and rest without any late gadolinium enhancement are interpreted as artifact. This algorithm improves the diagnostic accuracy over interpretation of the perfusion images alone [40].

While this approach is usually sufficient for most diagnostic purposes, it has limitations. First, because no actual numeric metric for perfusion is calculated, it is difficult to compare scans longitudinally over time or in a cross-section between different subjects. Second, because perfusion defects represent relative reductions in blood flow with respect to the best-perfused region of the myocardium, assessment of relative perfusion alone may result in either an over- or underestimation of myocardial perfusion, or a failure to recognize diffuse limitations in flow reserve, which can be seen in multi-vessel coronary artery disease or diffuse microvascular dysfunction. Lastly, without being able to use numeric thresholds, there is considerable subjectivity in determining what is normal vs abnormal perfusion, which can introduce bias into measurements. For these reasons, there has been a great deal of effort towards quantifying cardiac perfusion measurements.



## Semi-quantitative

Broadly speaking, semi-quantitative approaches result in numeric indices of perfusion, but the units of the measurement are not synonymous with blood flow (i.e. not ml/min/g). For example, the qualitative approach described above could be modified by comparing the change in signal in diseased myocardium versus the change in signal in healthy myocardium in the same subject. While this ratio will give a numeric value, it will not be units of blood flow. In general, while semi-quantitative approaches do allow for some statistical comparisons to be made, they are still limited compared to a true quantitative approach. The measurements themselves often depend on non-flow related parameters such as contrast dose or coil sensitivity, so there can still be problems comparing across subjects and over time. Additionally, because units are not in ml/min/g, direct comparisons cannot be made to other imaging modalities that are truly quantitative. For example, blood flow measured by PET or microspheres would not be directly comparable to MRI signal ratios. In experimental models, semiquantitative perfusion indices have been shown to underestimate myocardial blood flow, especially in hyperemic zones [41].

Of the semi-quantitative approaches, one of the most common ones is measuring the upslope of the signal intensity

curve in the myocardium (Fig. 13.6). Because only the upslope is measured, this method is dependent wholly on the contrast wash-in and is insensitive to contrast wash-out. During the wash-in, changes in tissue relaxivity are due principally to incoming contrast agent from arterial blood, and the rate of incoming contrast will be proportional to blood flow. However, most contrast agents used in CMR are not intravascular and will leak into the extravascular space, and additionally there is significant spin exchange between intravascular and extravascular compartments. Both of these effects complicate interpretation of relaxivity changes during the wash-out period. By using only the wash-in period, upslope measurement largely avoids these concerns. Because upslope measurement does not give units of flow, it is not an absolute quantitative approach. However, upslope of the AIF is often used to normalize between scans, and a recent publication [42] has suggested that calibrating global upslope (measured across the entire LV) to global flow (measured at the coronary sinus) may allow for absolute quantification.

## Absolute Quantification: Theory

Absolute quantification approaches aim to measure not just a perfusion related parameter but an exact measurement of

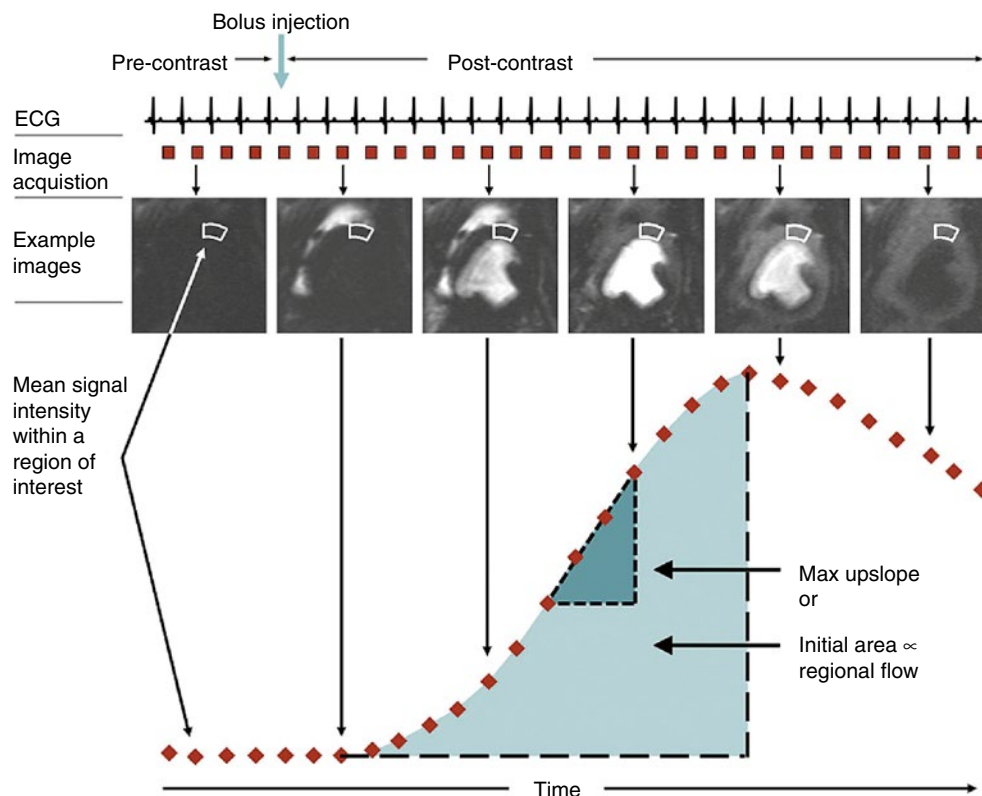


**Fig. 13.6** Peak upslope or area under the curve are often used as semi-quantitative ways to measure perfusion (Reproduced from Lee and Johnson [39], with permission of Elsevier)

perfusion in ml of blood, per minute of time, per gram of myocardium (ml/min/g). These approaches all make use of kinetic modeling and input functions.

The fundamental model for quantitative perfusion imaging in any organ system is

$$C(t) = BF \cdot (AIF(t) \otimes R(t))$$

Where  $C(t)$  is the contrast in the tissue,  $BF$  is the blood flow in the tissue,  $AIF(t)$  is the arterial input function, and  $R(t)$  is the residue function.  $AIF(t)$  is the contrast in the feeding artery, so  $BF \cdot AIF(t)$  describes the amount of contrast that is flowing into the tissue. In CMR perfusion, the AIF is typically sampled in the left ventricular blood pool. The residue function,  $R(t)$ , is a measure of contrast retention in the tissue.  $R(t)$  can also be thought of as the tissue response to a short bolus of contrast directly in the feeding artery, and it is analogous to an impulse response function.  $\otimes$  is the convolution function, defined by

$$f(t) \otimes g(t) = \int_{-\infty}^{\infty} f(\tau) g(t - \tau) d\tau$$

The aim of absolute quantification is to solve the first equation for  $BF$ . However, only  $C(t)$  and  $AIF(t)$  can be measured directly. To find  $BF$ ,  $R(t)$  must be found by deconvolving  $AIF(t)$  from  $C(t)$ . Once  $BF \cdot R(t)$  is found,  $BF$  is measured as the maximum of the  $BF \cdot R(t)$  curve ( $R(t)$  is defined as having a max of 1, so the maximum of  $BF \cdot R(t)$  will be  $BF$ ) (Fig. 13.7).

There are a number of possible methods for deconvolving an AIF from a measured signal. With a model-dependent approach, there is an assumed general shape for  $R(t)$  that is described by a few parameters (typically a Fermi function), and finding  $R(t)$  essentially becomes a fitting problem to find the parameters for  $R(t)$  that cause  $AIF(t) \otimes R(t)$  to best fit the experimental data. Another popular variation on a model-dependent approach is to use compartment models. In compartment models, a system of differential equations that depends on blood flow is used to describe contrast flow between various compartments (e.g. intravascular, extracellular). With a model-independent approach, no assumptions whatsoever are made about the shape of  $R(t)$ , and finding

$R(t)$  is done mathematically via regularized inverse Fourier transformations or singular value decomposition (SVD). For cardiac perfusion, the most popular approaches are Fermi function and two compartment models.

### Absolute Quantification: AIF Selection

Accurately deconvolving the AIF and finding the correct residue function requires an accurate sampling of the AIF. While it is easy to locate the AIF in CMR – it is easily sampled in the LV – it is difficult to accurately capture the correct shape of the AIF. First, the AIF peak is very sharp since the contrast passes through the LV so quickly, and most acquisition schemes will miss the exact top of the peak. To account for this, many processing algorithms assume the AIF is described by a gamma variate function [43] and will use the sampled AIF data to fit a continuous gamma variate that is then used in the rest of the algorithm. Second, because the concentration of contrast is so high in the LV during the first pass of the bolus, there are significant saturation and  $T_2^*$  effects, which manifest as flattening the measured AIF (Fig. 13.8). This problem is much more difficult to correct, and there have been a number of proposed methods to remedy it. One method which has gained much attention is the dual-bolus method.

In a dual bolus scheme, there are two separate injections of the contrast agent. The first dose is small and is used only for measuring the AIF. The second dose is larger (typically 4–10× larger) and is used to measure the contrast uptake in the tissue. Because the first dose is so small, many of the saturation and non-linear effects from high contrast concentration are avoided, so the sampled AIF better represents the true shape of the bolus passage through the LV. The AIF from the large bolus is then calculated from the measured AIF from the smaller bolus (Fig. 13.9). This constructed AIF is then used to deconvolve signal curves from the tissue during passage of the larger bolus. Because the second dose is so much larger, the effects on the tissue from any remaining contrast from the first dose can be ignored. Dual bolus has been validated against microspheres [41] but it can be difficult to implement. Without a second separate injector for the smaller bolus (which is not available in many imaging cen-

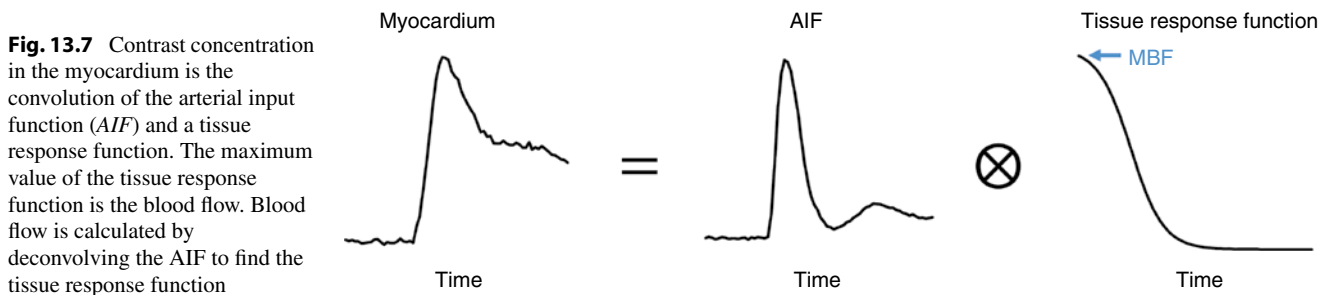


**Fig. 13.8** Signal intensity of central k-space lines vs  $R_1$  for a SR prepared FLASH sequence (signal equation can be derived similarly to the FLASH equation with no preparation. See any MRI sequence textbook, e.g. Haacke et al. for a FLASH signal derivation). For low doses of contrast, the signal response is linear, but at higher doses there is significant non-linearity

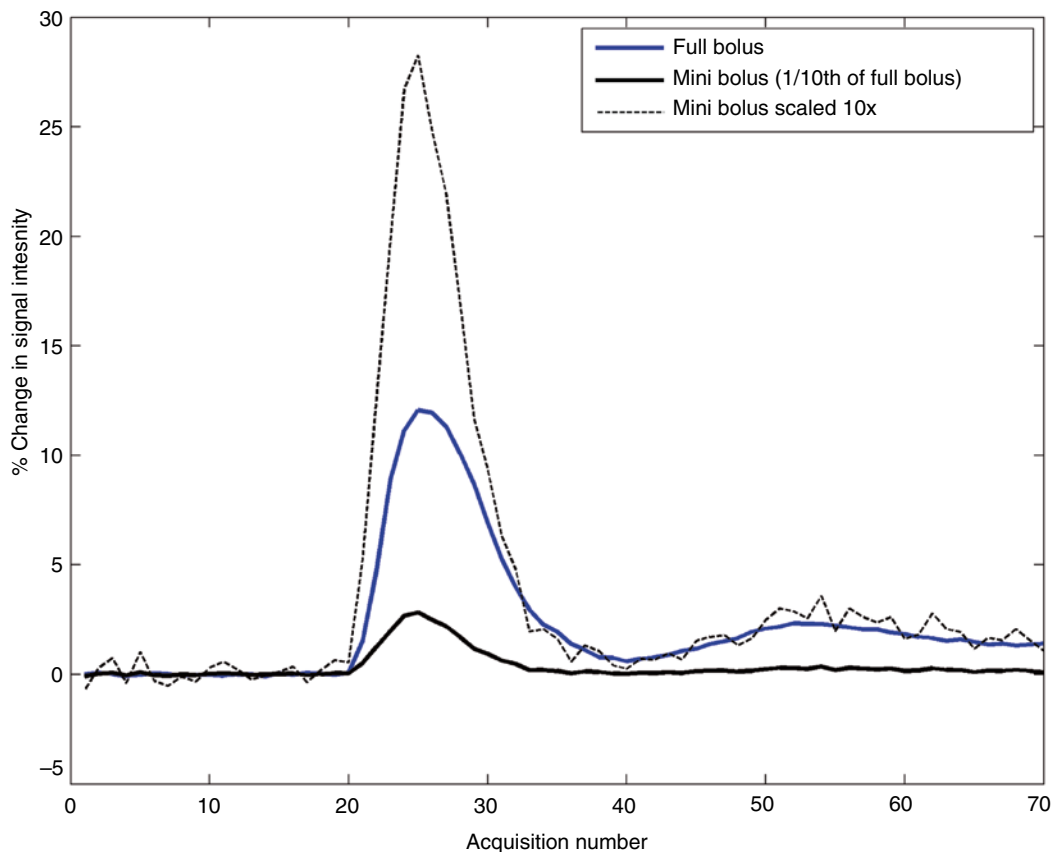
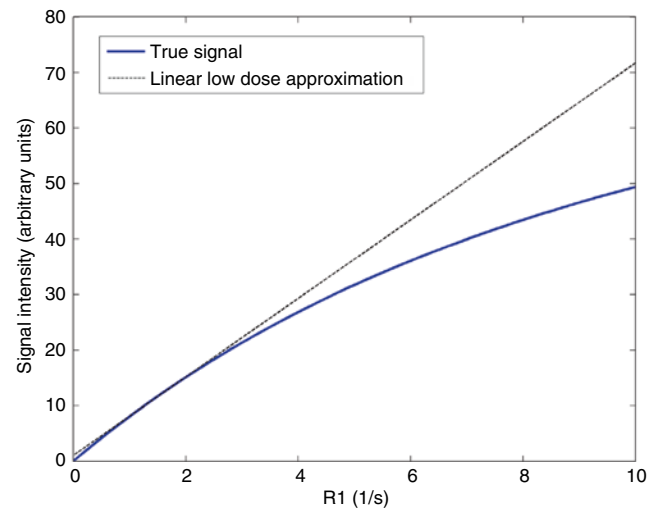


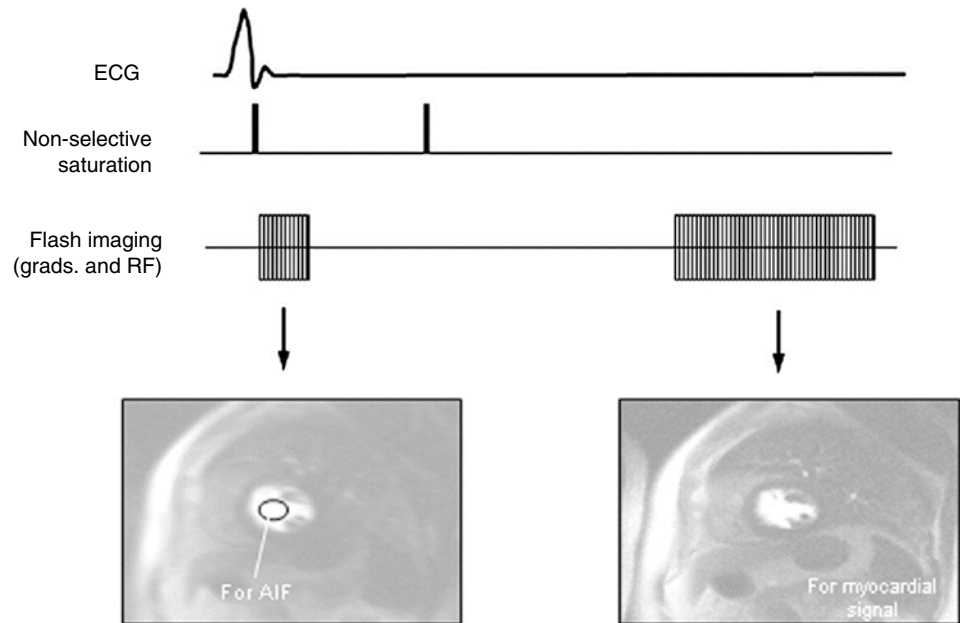
**Fig. 13.9** AIF for a full bolus, a bolus diluted to one tenth full dose, and the one tenth dose scaled up 10x. Note that the full bolus has a significantly lower peak than the scaled mini-bolus

ters), using one injector to administer both boluses can be technically challenging.

Other approaches have been suggested that do not rely on separate contrast injections. Like dual bolus schemes, dual sequence [44] schemes also use the principle of measuring the AIF and tissue uptake separately. However, instead of

using a separate bolus to measure the AIF, with dual sequence there is a special slice selected during acquisition that is meant solely for measuring the AIF (Fig. 13.10). This slice is acquired with different imaging parameters (lower resolution, short TE, short TI) that minimize non-linearity and  $T_2^*$  effects. Another recently proposed method uses

**Fig. 13.10** Dual sequence method for measuring AIF. One low resolution slice is imaged with short TE and TI and is intended solely for measuring the AIF (Reproduced from Gatehouse et al. [44], with permission of John Wiley & Sons)



constrained modeling to estimate the input function from the tissue curves and requires neither a separate bolus nor acquisition [45].

## Future Directions

Cardiac perfusion MRI is a rapidly evolving field, and there are a number of emerging techniques. We conclude the chapter by briefly discussing just a few of them.

## Myocardial Non-linearity

Considerable attention has been paid to the non-linearity of the arterial input function. However, less commonly investigated are the effects of non-linearity on the myocardial signal. It is sometimes assumed that there is no myocardial saturation because the total signal in a myocardial voxel is not saturated, but this is not true. While not all of the voxel is saturated, the part of the voxel composed of blood may be saturated, which would introduce non-linear effects into the myocardial signal even if the total signal intensity is much less than that of pure blood. Some models have been proposed for correcting myocardial saturation [46, 47], but research is still ongoing.

## ASL

The vast majority of cardiac perfusion scans use a contrast bolus as described above. However, some groups have also used arterial spin labeling (ASL) as alternative to contrast

administration. In general, ASL has worse CNR than bolus first-pass, but because it does not use injected contrast agent the number of acquisitions is not limited by contrast dose, and concerns about nephrogenic systemic sclerosis are avoided. At this time, ASL remains mostly an experimental method for MR cardiac perfusion, but it has been used in both animals [48–51] and humans [52–54].

## BOLD

Like ASL, blood oxygenation level dependent (BOLD) imaging is another experimental cardiac perfusion technique that requires no exogenous contrast and is minimally invasive. Used extensively in functional MRI (fMRI) neuroimaging, the BOLD effect relies on  $T_2$  differences between oxygenated and deoxygenated hemoglobin. Unlike ASL or contrast imaging, BOLD signal is proportional to blood oxygenation, not blood flow. The two are often related, however, and changes in BOLD signal have been shown by some groups to be associated with coronary artery disease in both humans [55, 56] and animal models [11, 57–60].

## Summary

Cardiac MRI is emerging as an alternative to SPECT for measuring cardiac perfusion that has many potentially important clinical applications. There are many options when designing a cardiac MRI sequence, including preparation, RF design, and image readout, and after collecting images there are still further options in how to analyze the data. For many of these choices there is no clear consensus

on which is best, and each decision has its own tradeoffs depending on the application. Cardiac perfusion MRI is the focus of much exciting research, and outside of the most commonly used contrast agent first-pass scans, there are a number of exciting newer techniques such as ASL, BOLD, and methods for absolute quantification that may improve how cardiac MRI is used in the clinic and lead to further advances in the diagnosis of cardiac disease.

## References

1. Stirrat J, White JA. The prognostic role of late gadolinium enhancement magnetic resonance imaging in patients with cardiomyopathy. *Can J Cardiol*. 2013;29(3):329–36.
2. Cook SC, Ferketich AK, Raman SV. Myocardial ischemia in asymptomatic adults with repaired aortic coarctation. *Int J Cardiol*. 2009;133(1):95–101.
3. Wang L, et al. Coronary risk factors and myocardial perfusion in asymptomatic adults: the Multi-Ethnic Study of Atherosclerosis (MESA). *J Am Coll Cardiol*. 2006;47(3):565–72.
4. Klocke FJ, et al. ACC/AHA/ASNC guidelines for the clinical use of cardiac radionuclide imaging – executive summary: a report of the American College of Cardiology/American Heart Association Task Force on Practice Guidelines (ACC/AHA/ASNC Committee to Revise the 1995 Guidelines for the Clinical Use of Cardiac Radionuclide Imaging). *J Am Coll Cardiol*. 2003;42(7):1318–33.
5. Jerosch-Herold M. Quantification of myocardial perfusion by cardiovascular magnetic resonance. *J Cardiovasc Magn Reson*. 2010;12:57.
6. Kellman P, Arai AE. Imaging sequences for first pass perfusion – a review. *J Cardiovasc Magn Reson*. 2007;9(3):525–37.
7. Coelho-Filho OR, et al. MR myocardial perfusion imaging. *Radiology*. 2013;266(3):701–15.
8. Gerber BL, et al. Myocardial first-pass perfusion cardiovascular magnetic resonance: history, theory, and current state of the art. *J Cardiovasc Magn Reson*. 2008;10:18.
9. Jerosch-Herold M, et al. Analysis of myocardial perfusion MRI. *J Magn Reson Imaging*. 2004;19(6):758–70.
10. Zhang H, et al. Accurate myocardial  $T_1$  measurements: toward quantification of myocardial blood flow with arterial spin labeling. *Magn Reson Med*. 2005;53(5):1135–42.
11. Wright KB, et al. Assessment of regional differences in myocardial blood flow using  $T_2$ -weighted 3D BOLD imaging. *Magn Reson Med*. 2001;46(3):573–8.
12. Tsekos NV, et al. Fast anatomical imaging of the heart and assessment of myocardial perfusion with arrhythmia insensitive magnetization preparation. *Magn Reson Med*. 1995;34(4):530–6.
13. Kim D, Cernicanu A, Axel L. B(0) and B(1)-insensitive uniform  $T(1)$ -weighting for quantitative, first-pass myocardial perfusion magnetic resonance imaging. *Magn Reson Med*. 2005;54(6):1423–9.
14. Kim D, et al. Comparison of the effectiveness of saturation pulses in the heart at 3T. *Magn Reson Med*. 2008;59(1):209–15.
15. Haase A, et al. Inversion recovery snapshot FLASH MR imaging. *J Comput Assist Tomogr*. 1989;13(6):1036–40.
16. Ding S, Wolff SD, Epstein FH. Improved coverage in dynamic contrast-enhanced cardiac MRI using interleaved gradient-echo EPI. *Magn Reson Med*. 1998;39(4):514–9.
17. Schreiber WG, et al. Dynamic contrast-enhanced myocardial perfusion imaging using saturation-prepared TrueFISP. *J Magn Reson Imaging*. 2002;16(6):641–52.
18. Fenchel M, et al. Multislice first-pass myocardial perfusion imaging: comparison of saturation recovery (SR)-TrueFISP-two-dimensional (2D) and SR-TurboFLASH-2D pulse sequences. *J Magn Reson Imaging*. 2004;19(5):555–63.
19. Lyne JC, et al. Direct comparison of myocardial perfusion cardiovascular magnetic resonance sequences with parallel acquisition. *J Magn Reson Imaging*. 2007;26(6):1444–51.
20. Sodickson DK, Manning WJ. Simultaneous acquisition of spatial harmonics (SMASH): fast imaging with radiofrequency coil arrays. *Magn Reson Med*. 1997;38(4):591–603.
21. Pruessmann KP, et al. SENSE: sensitivity encoding for fast MRI. *Magn Reson Med*. 1999;42(5):952–62.
22. Griswold MA, et al. Generalized autocalibrating partially parallel acquisitions (GRAPPA). *Magn Reson Med*. 2002;47(6):1202–10.
23. Tsao J, Boesiger P, Pruessmann KP. k-t BLAST and k-t SENSE: dynamic MRI with high frame rate exploiting spatiotemporal correlations. *Magn Reson Med*. 2003;50(5):1031–42.
24. Mistretta CA, et al. Highly constrained backprojection for time-resolved MRI. *Magn Reson Med*. 2006;55(1):30–40.
25. Ge L, et al. Myocardial perfusion MRI with sliding-window conjugate-gradient HYPR. *Magn Reson Med*. 2009;62(4):835–9.
26. Kozerke S, Tsao J. Reduced data acquisition methods in cardiac imaging. *Top Magn Reson Imaging*. 2004;15(3):161–8.
27. Grist TM, et al. Time-resolved angiography: past, present, and future. *J Magn Reson Imaging*. 2012;36(6):1273–86.
28. Deshmane A, et al. Parallel MR imaging. *J Magn Reson Imaging*. 2012;36(1):55–72.
29. Pedersen H, et al. Quantification of myocardial perfusion using free-breathing MRI and prospective slice tracking. *Magn Reson Med*. 2009;61(3):734–8.
30. Milles J, et al. Fully automated motion correction in first-pass myocardial perfusion MR image sequences. *IEEE Trans Med Imaging*. 2008;27(11):1611–21.
31. Stegmann MB, Olafsdottir H, Larsson HB. Unsupervised motion-compensation of multi-slice cardiac perfusion MRI. *Med Image Anal*. 2005;9(4):394–410.
32. Bidaut LM, Vallee JP. Automated registration of dynamic MR images for the quantification of myocardial perfusion. *J Magn Reson Imaging*. 2001;13(4):648–55.
33. Yang GZ, et al. Motion and deformation tracking for short-axis echo-planar myocardial perfusion imaging. *Med Image Anal*. 1998;2(3):285–302.
34. Scott AD, Keegan J, Firmin DN. Motion in cardiovascular MR imaging. *Radiology*. 2009;250(2):331–51.
35. Di Bella EV, Parker DL, Sinusas AJ. On the dark rim artifact in dynamic contrast-enhanced MRI myocardial perfusion studies. *Magn Reson Med*. 2005;54(5):1295–9.
36. Sharma P, et al. Effect of Gd-DTPA-BMA on blood and myocardial  $T_1$  at 1.5T and 3T in humans. *J Magn Reson Imaging*. 2006;23(3):323–30.
37. Kim D, Axel L. Multislice, dual-imaging sequence for increasing the dynamic range of the contrast-enhanced blood signal and CNR of myocardial enhancement at 3T. *J Magn Reson Imaging*. 2006;23(1):81–6.
38. Noeske R, et al. Human cardiac imaging at 3 T using phased array coils. *Magn Reson Med*. 2000;44(6):978–82.
39. Lee DC, Johnson NP. Quantification of absolute myocardial blood flow by magnetic resonance perfusion imaging. *JACC Cardiovasc Imaging*. 2009;2(6):761–70.
40. Klem I, et al. Improved detection of coronary artery disease by stress perfusion cardiovascular magnetic resonance with the use of delayed enhancement infarction imaging. *J Am Coll Cardiol*. 2006;47(8):1630–8.
41. Christian TF, et al. Absolute myocardial perfusion in canines measured by using dual-bolus first-pass MR imaging. *Radiology*. 2004;232(3):677–84.
42. Aquaro GD, et al. A fast and effective method of quantifying myocardial perfusion by magnetic resonance imaging. *Int J Cardiovasc Imaging*. 2013;29(6):1313–24.

43. Thompson Jr HK, et al. Indicator transit time considered as a gamma variate. *Circ Res.* 1964;14:502–15.
44. Gatehouse PD, et al. Accurate assessment of the arterial input function during high-dose myocardial perfusion cardiovascular magnetic resonance. *J Magn Reson Imaging.* 2004;20(1):39–45.
45. Fluckiger JU, et al. Absolute quantification of myocardial blood flow with constrained estimation of the arterial input function. *J Magn Reson Imaging.* 2013;38(3):603–9.
46. Cernicanu A, Axel L. Theory-based signal calibration with single-point  $T_1$  measurements for first-pass quantitative perfusion MRI studies. *Acad Radiol.* 2006;13(6):686–93.
47. Hsu LY, Kellman P, Arai AE. Nonlinear myocardial signal intensity correction improves quantification of contrast-enhanced first-pass MR perfusion in humans. *J Magn Reson Imaging.* 2008;27(4):793–801.
48. Jacquier A, et al. Quantification of myocardial blood flow and flow reserve in rats using arterial spin labeling MRI: comparison with a fluorescent microsphere technique. *NMR Biomed.* 2011;24(9):1047–53.
49. Troalen T, et al. Cine-ASL: a steady-pulsed arterial spin labeling method for myocardial perfusion mapping in mice. Part I. Experimental study. *Magn Reson Med.* 2013;70(5):1389–98.
50. Abeykoon S, Sargent M, Wansapura JP. Quantitative myocardial perfusion in mice based on the signal intensity of flow sensitized CMR. *J Cardiovasc Magn Reson.* 2012;14:73.
51. McCommis KS, et al. Feasibility study of myocardial perfusion and oxygenation by noncontrast MRI: comparison with PET study in a canine model. *Magn Reson Imaging.* 2008;26(1):11–9.
52. Zun Z, Wong EC, Nayak KS. Assessment of myocardial blood flow (MBF) in humans using arterial spin labeling (ASL): feasibility and noise analysis. *Magn Reson Med.* 2009;62(4):975–83.
53. Northrup BE, et al. Resting myocardial perfusion quantification with CMR arterial spin labeling at 1.5 T and 3.0 T. *J Cardiovasc Magn Reson.* 2008;10:53.
54. Do HP, Jao TR, Nayak KS. Myocardial arterial spin labeling perfusion imaging with improved sensitivity. *J Cardiovasc Magn Reson.* 2014;16(1):15.
55. Walcher T, et al. Myocardial perfusion reserve assessed by  $T_2$ -prepared steady-state free precession blood oxygen level-dependent magnetic resonance imaging in comparison to fractional flow reserve. *Circ Cardiovasc Imaging.* 2012;5(5):580–6.
56. Arnold JR, et al. Myocardial oxygenation in coronary artery disease: insights from blood oxygen level-dependent magnetic resonance imaging at 3 tesla. *J Am Coll Cardiol.* 2012;59(22):1954–64.
57. Shea SM, et al.  $T_2$ -prepared steady-state free precession blood oxygen level-dependent MR imaging of myocardial perfusion in a dog stenosis model. *Radiology.* 2005;236(2):503–9.
58. Tsaftaris SA, et al. Ischemic extent as a biomarker for characterizing severity of coronary artery stenosis with blood oxygen-sensitive MRI. *J Magn Reson Imaging.* 2012;35(6):1338–48.
59. Ghugre NR, et al. Myocardial BOLD imaging at 3 T using quantitative  $T_2$ : application in a myocardial infarct model. *Magn Reson Med.* 2011;66(6):1739–47.
60. Fieno DS, et al. Myocardial perfusion imaging based on the blood oxygen level-dependent effect using  $T_2$ -prepared steady-state free-precession magnetic resonance imaging. *Circulation.* 2004;110(10):1284–90.